Does Model Parameter Error Cause a Significant "Spring Predictability Barrier" for El Niño Events in the Zebiak–Cane Model?

YANSHAN YU AND MU MU

Key Laboratory of Ocean Circulation and Waves, Institute of Oceanology, Chinese Academy of Sciences, Qingdao, China

WANSUO DUAN

LASG, Institute of Atmospheric Physics, Chinese Academy of Sciences, Beijing, China

(Manuscript received 24 August 2010, in final form 16 July 2011)

ABSTRACT

Within the framework of the Zebiak–Cane model, the approach of conditional nonlinear optimal perturbation (CNOP) is used to study the effect of model parameter errors on El Niño–Southern Oscillation (ENSO) predictability. The optimal model parameter errors are obtained within a reasonable error bound (i.e., CNOP-P errors), which have the largest effect on the results of El Niño predictions. The resultant prediction errors were investigated in depth. The CNOP-P errors do not cause a noticeable prediction error of the sea surface temperature anomaly averaged over the Niño-3 region and do not show an obvious season-dependent evolution of the prediction errors. Consequently, the CNOP-P errors do not cause a significant spring predictability barrier (SPB) for El Niño events. In contrast, the initial errors that have the largest effect on the results of the predictions (i.e., the CNOP-I errors) show a season-dependent evolution, with the largest error increase in spring, and also cause a large prediction error, thereby generating a significant SPB. The initial errors play a more important role than the parameter errors in generating a significant SPB for El Niño events. To further validate this result, the authors investigated the situation in which CNOP-I and CNOP-P errors are simultaneously superimposed in the model, which may be a more credible approach because the initial errors and model parameter errors coexist under realistic predictions. The combined mode of CNOP-I and CNOP-P errors shows a similar season-dependent evolution to that of CNOP-I errors and yields a large prediction error, thereby inducing a significant SPB. The inference, therefore, is that initial errors play a more important role than model parameter errors in generating a significant SPB for El Niño predictions of the Zebiak–Cane model. This result helps to clarify the roles of the initial error and parameter error in the development of an SPB, and highlights the role of initial errors, which demonstrates that the SPB could be markedly reduced by improving the initial conditions. The results provide a theoretical basis for improving data assimilation in ENSO predictions.

1. Introduction

The El Niño–Southern Oscillation (ENSO) cycle has attracted the attention of scientists in recent decades because its environmental and socioeconomic impacts are felt worldwide (e.g., McPhaden et al. 2006). Knowledge of the ENSO cycle and forecasts of its variations are valuable for the agricultural sector, public health and safety, and many other climate-sensitive human endeavors.

Since the development of the Zebiak–Cane model (Zebiak and Cane 1987: hereafter the ZC model), which for the first time demonstrated the possibility of ENSO prediction by forecasting the 1986/87 El Niño event in real time, a suite of models with varying degrees of complexity has been developed for ENSO predictions (Neelin 1990; Kleeman 1991; Latif et al. 1993; Penland and Magorian 1993; Luo et al. 2008). Significant advances in ENSO theories and predictions have been made in recent decades, particularly through the Tropical Ocean Global Atmosphere (TOGA) program [see the review by Wang and Picaut (2004)]; however, there remain considerable uncertainties in realistic ENSO predictions (Jin et al. 2008). In particular, if forecasts are made before and across the boreal spring season, the

Corresponding author address: Wansuo Duan, LASG, Institute of Atmospheric Physics, Chinese Academy of Sciences, P.O. Box 9804, Beijing 100029, China.
E-mail: duanws@lasg.iap.ac.cn

DOI: 10.1175/2011JCLI4022.1

forecast skill tends to show a significant drop during this season, which has been termed the ''spring predictability barrier'' (SPB) of ENSO (Yu and Kao 2007).

The SPB is a well-known characteristic of ENSO forecasts (Webster and Yang 1992; Lau and Yang 1996; McPhaden 2003) and exists in both coupled and statistical models. In some cases, the SPB is even stronger in statistical models than in general circulation models (GCMs) (van Oldenborgh et al. 2005). Previous studies have investigated the SPB phenomenon from the viewpoint of initial error growth, revealing that the SPB phenomenon in ENSO forecasting is related to a large prediction error; in particular, prominent error growth occurs during spring in the case when the prediction is made prior to this season (Mu et al. 2007a,b; Duan et al. 2009; Yu et al. 2009). Moore and Kleeman (1996) investigated the SPB by tracing the evolution of the linear singular vector (LSV) (Lorenz 1965), which has also been used to investigate other problems of ENSO predictability (Blumenthal 1991; Xue et al. 1997; Thompson 1998). Chen et al. (1995, 2004) showed that the SPB could be greatly reduced by improving the model initialization and Mu et al. (2007b) used a nonlinear technique of conditional nonlinear optimal perturbation (CNOP) to investigate the SPB for ENSO events in the ZC model, revealing that the CNOP initial (CNOP-I) errors cause a significant SPB for El Niño events. Duan et al. (2009) and Yu et al. (2009) identified two types of CNOP-I errors that induce a significant SPB and proposed two different dynamical mechanisms of error growth related to the SPB for El Niño events. Furthermore, Yu et al. pointed out that the CNOP-I errors possess a large-scale zonal dipolar pattern of the sea surface temperature anomaly (SSTA) component similar to LSV errors, but the former covers a broader region than the latter, which leads to a significant difference in their resultant prediction errors and then indicates that the sensitivity of the prediction results to initial uncertainties. Yu et al. (2009) also showed that random initial errors without particular spatial patterns fail to cause a SPB. Based on these previous works, it can be inferred that the occurrence of the SPB is closely related to the spatial pattern of initial errors.

Prediction uncertainties are generally caused by initial errors and model errors. In realistic predictions of ENSO, the SPB phenomenon commonly appears when both initial and model errors occur in the model. Furthermore, an increasing number of studies have indicated that model errors influence the ability to forecast ENSO (Wu et al. 1993; Hao and Ghil 1994; Blanke et al. 1997; Flugel and Chang 1998; Latif et al. 1998; Liu 2002; Zhang et al. 2003; Zavala-Garay et al. 2004; Williams 2005). The model errors may arise from various schemes of physical parameterizations (Syu and Neelin 2000), atmospheric noise, or other high frequency variations such as westerly wind bursts and the Madden–Julian oscillation (Gebbie et al. 2007; Tang and Yu 2008; Marshall et al. 2009). Some of these processes are omitted in intermediate-complexity models (Zebiak and Cane 1987; McCreary and Anderson 1991).

Another important source of model errors are uncertainties in empirical model parameters (Mu et al. 2002). Previous studies have investigated the effect of such uncertainties on the modulation of ENSO events by systematically varying the values of relevant parameters in controlled experiments. For example, Zebiak and Cane (1987) explored the sensitivity of ENSO irregularity to parameter perturbations, revealing the importance of accurate values of parameters for ENSO simulations. Kirtman (1997) found that the ratio of the atmospheric to oceanic Rossby radii of deformation has a strong effect on the meridional structure of oceanic Rossby waves, thereby influencing the period of ENSO. MacMynowski and Tziperman (2008) also reported the sensitivity of ENSO's period to various parameters.

The results of these studies indicate that parameter uncertainties have an effect on ENSO simulations. ENSO simulations are generally described by a long-term integration of the given model; however, in recent studies, realistic ENSO predictions have focused on short-term climate predictions with lead times from one month to one year, although several ENSO hindcast experiments employed a lead time of 2 yr (Kirtman et al. 2002; Jin et al. 2008). In this context, it is natural to assess 1) the effect of model parameter errors on El Niño predictions, 2) whether the model parameter errors cause a significant SPB, and 3) which errors (i.e., initial or model parametric) contribute most to the generation of a significant SPB.

Mu et al. (2010) extended the CNOP approach to include both optimal initial perturbations (CNOP-I) and optimal model parameter perturbations (CNOP-P). This renewed CNOP approach can be used to study not only the predictability associated with initial errors but also that related to model parameter errors. Furthermore, it enables investigations of the relative effects of initial errors and model parameter errors on prediction uncertainties and of the dominant source of the uncertainties that have a large influence on predictability (Duan and Zhang 2010). In the present study, we use the CNOP approach to identify the errors that play a dominant role in the generation of SPB for El Niño events.

The remainder of this paper is organized as follows. In section 2, we briefly describe the CNOP approach and, in section 3 calculate the CNOP-P error, investigate the seasonal evolution of the prediction errors caused by the

CNOP-P error, and study the effect of parameter errors on the development of a significant SPB for El Niño events. In section 4, we compare the prediction errors caused by CNOP-I and CNOP-P errors and identify the errors that play a dominant role in generating a significant SPB. Finally, a discussion and summary are presented in section 5.

2. Conditional nonlinear optimal perturbation

The CNOP approach, developed to identify the optimal initial perturbation in a given constraint, has been used to study the predictability of ENSO events (Mu and Duan 2003; Duan et al. 2004, 2008; Duan and Mu 2006; Mu et al. 2007a,b), to assess the sensitivity of ocean circulation (Mu et al. 2004; Sun et al. 2005; Wu and Mu 2009; Terwisscha van Scheltinga and Dijkstra 2008), and to identify sensitive areas for typhoon observations (Mu et al. 2009). These studies demonstrated the usefulness of the CNOP-I approach in analyses of weather and climate predictability.

Existing numerical models are unable to describe exactly the atmospheric and oceanic motions, and contain model errors. An important source of model errors are uncertainties in model parameters (Lu and Hsieh 1998; Mu et al. 2002). This gives rise to the question of how to estimate the predictability limit related to the error modes of the model parameters. To address this question, Mu et al. (2010) extended the CNOP approach to include not only CNOP-I but also the optimal model parameter perturbation (CNOP-P). In the present study, we use this renewed approach to study the SPB for El Niño events. The CNOP approach is briefly described below.

We write the evolution equations for the state vector $\mathbf{w}$ as follows:

$$\begin{cases} \dfrac{\partial \mathbf{w}}{\partial t} + \mathbf{F}(\mathbf{w}, \mathbf{p}, t) = 0 \\ \mathbf{w}|_{t=0} = \mathbf{w}_0, \end{cases} \tag{1}$$

where $\mathbf{w}(\mathbf{x}, t) = [w_1(\mathbf{x}, t), w_2(\mathbf{x}, t), \ldots, w_l(\mathbf{x}, t)]$ consists of l state variables (e.g., thermocline depth anomalies and SST anomalies; $\mathbf{w}_0$ is the initial state; $\mathbf{x} = (x_1, x_2, \ldots, x_n)$, where $\mathbf{x} \in \Omega$ and Ω is a domain in R^n; t is time, with $0 \leq t < \infty$; $\mathbf{p} = (p_1, p_2, \ldots, p_m)$ is the model parameter vector; and $\mathbf{F}$ is a nonlinear operator.

Assuming that the dynamical system equation and the initial state are known exactly, the future state can be determined by integrating Eq. (1) with the appropriate initial condition. The solution to Eq. (1) for the state vector $\mathbf{w}$ at time τ is given as

$$\mathbf{w}(\mathbf{x}, \tau) = M_\tau(\mathbf{p})(\mathbf{w}_0), \tag{2}$$

where $M_\tau(\mathbf{p})$ is the propagator of Eq. (1), with the parameter vector $\mathbf{p}$. The term $M_\tau(\mathbf{p})$ propagates the initial value to time τ in the future, as described by Eq. (2).

The solutions of Eq. (2) are $\mathbf{U}(t)$ and $\mathbf{U}(t) + \mathbf{u}(t)$, with initial values $\mathbf{U}_0$ and $\mathbf{U}_0 + \mathbf{u}_0$. Thus, we have

$$\mathbf{U}(\tau) = M_\tau(\mathbf{p})(\mathbf{U}_0), \quad \mathbf{U}(\tau) + \mathbf{u}_I(\tau) = M_\tau(\mathbf{p})(\mathbf{U}_0 + \mathbf{u}_0), \tag{3}$$

where $\mathbf{u}_0$ is the initial perturbation of a time-dependent state $\mathbf{U}(t)$ (hereafter the reference state) and $\mathbf{u}_I(\tau)$ describes the nonlinear evolution of the initial perturbation.

In addition, while assuming that the parameter perturbation vector $\mathbf{p}'$ is superimposed on the parameter vector $\mathbf{P}$, we obtain

$$\mathbf{U}(\tau) = M_\tau(\mathbf{P})(\mathbf{U}_0), \quad \mathbf{U}(\tau) + \mathbf{u}_p(\tau) = M_\tau(\mathbf{P} + \mathbf{p}')(\mathbf{U}_0) \tag{4}$$

In which $\mathbf{u}_p(\tau)$ describes the departure from the reference state $\mathbf{U}(\tau)$ caused by $\mathbf{p}'$.

Considering the existence of both an initial perturbation and parameter perturbation in Eq. (2), we have

$$\begin{aligned} \mathbf{U}(\tau) &= M_\tau(\mathbf{P})(\mathbf{U}_0), \\ \mathbf{U}(\tau) + \mathbf{u}_{I,p}(\tau) &= M_\tau(\mathbf{P} + \mathbf{p}')(\mathbf{U}_0 + \mathbf{u}_0), \end{aligned} \tag{5}$$

where $\mathbf{u}_{I,p}(\tau)$ is the departure from the reference state $\mathbf{U}(\tau)$ caused by the combined mode of the initial and model parameter perturbations.

The nonlinear optimization problem is defined as

$$J_1(\mathbf{u}_{0\delta}, \mathbf{p}'_\sigma) = \max_{\mathbf{u}_0 \in C_\delta, \mathbf{p}' \in C_\sigma} J(\mathbf{u}_0, \mathbf{p}'), \tag{6}$$

where

$$J(\mathbf{u}_0, \mathbf{p}') = \|M_\tau(\mathbf{P} + \mathbf{p}')(\mathbf{U}_0 + \mathbf{u}_0) - M_\tau(\mathbf{P})(\mathbf{U}_0)\|,$$

where $\mathbf{u}_0$ and $\mathbf{p}'$ are perturbation vectors superimposed on the initial value of the reference state $\mathbf{U}_0$ and the parameter $\mathbf{P}$, respectively, with $\mathbf{u}_0 \in C_\delta, \mathbf{p}' \in C_\sigma$ as the constraint conditions. By solving Eq. (6), we obtain the optimal combined mode of the initial perturbation and parameter perturbation, $(\mathbf{u}_{0\delta}; \mathbf{p}'_\sigma)$, for a given constraint that induces the largest departure from the reference state $\mathbf{U}(t)$ at time τ. Mu et al. (2010) called this optimal combined mode CNOP, which has two special cases. The first is CNOP-I, denoted by $\mathbf{u}_{0\delta,I}$, which represents the initial perturbation with the largest nonlinear evolution at the prediction time and is obtained by solving the following optimization problem:

$$J_{u_0}(\mathbf{u}_{0\delta,I}) = \max_{\mathbf{u}_0 \in C_\delta} \|M_\tau(\mathbf{P})(\mathbf{U}_0 + \mathbf{u}_0) - M_\tau(\mathbf{P})(\mathbf{U}_0)\|. \tag{7}$$

The second case is CNOP-P, denoted by $\mathbf{p}'_{\sigma,p}$, which describes the parameter perturbation that results in the largest departure from a given reference state and can be obtained by evaluating the following optimization problem:

$$J_b(\mathbf{p}'_{\sigma,p}) = \max_{\mathbf{p}' \in C_\sigma} \|M_\tau(\mathbf{P} + \mathbf{p}')(\mathbf{U}_0) - M_\tau(\mathbf{P})(\mathbf{U}_0)\|. \tag{8}$$

Physically, CNOP represents the optimal combined mode of the initial error and the model parameter error, while CNOP-I, in perfect model experiments, acts as the optimal initial error, and CNOP-P, in experiments with perfect initial conditions, represents the optimal parameter error. In their respective scenarios, these cases cause the largest prediction error. In addition, the CNOP approach can be used to identify the errors that play a dominant role in yielding predictions with large uncertainties.

In this paper, the CNOP-I and CNOP-P errors of the ZC model are computed to investigate the major source of the uncertainties that yields a significant SPB, which is identified by comparing the results derived from the CNOP-I errors, the CNOP-P errors, and the combined mode of CNOP-I and CNOP-P errors. In fact, a comparison of CNOP errors with CNOP-I errors or with CNOP-P errors would be the preferred approach; however, one cannot successfully obtain CNOP by using existing solvers owing to different kinds of constraints for initial perturbation and parameter perturbation, despite that these solvers can be used to effectively compute CNOP-I and CNOP-P. Therefore, in this paper, we must consider the approximate combined mode of the CNOP-I and CNOP-P errors and compare it with CNOP-I or CNOP-P errors so as to identify the errors that play a dominant role in generating a significant SPB for El Niño events.

To calculate the CNOP-I and CNOP-P errors, we transform the corresponding maximization optimization problem into a minimization problem by considering the negative of the cost function. Then, existing solvers, such as the spectral projected gradient 2 (SPG2) (Birgin et al. 2000), sequential quadratic programming (SQP) (Powell 1982), and limited-memory Broyden–Fletcher–Goldfarb–Shanno (L-BFGS) (Liu and Nocedal 1989), can be used to compute CNOP-I and CNOP-P. The use of these solvers requires the gradient of the modified cost function with respect to the initial or parameter perturbation. In large-scale computations, the adjoint of the corresponding model is often used to obtain the gradient. Le Dimet and Talagrand (1986) described how to use an adjoint model to compute the gradient of the cost function with respect to the initial perturbation, while Mu et al. (2010) showed how to adopt this adjoint model to obtain the gradient of a cost function with respect to parameter perturbations. As such, the gradient of the cost function with respect to parameter perturbations can be obtained by using the adjoint approach.

Making use of information on the gradient with respect to both initial perturbation and parameter perturbations, the optimization solvers mentioned above are generally used to determine the minimum of the modified cost function [i.e., the maximum of the cost functions in the optimization problems presented in Eqs. (7) and (8)] along the direction of the gradient. In a phase space, the point corresponding to the minimum of the modified cost function represents either CNOP-I or CNOP-P.

3. Does CNOP-P error cause a significant SPB for El Niño events in the ZC model?

The ZC model is a nonlinear anomaly model of intermediate complexity that describes anomalies of a specified seasonally varying background, thus avoiding the ''climate drift'' problem (Zebiak and Cane 1987). The atmospheric model is a gridpoint model with a zonal resolution of 5.625° × 2.0°. The ocean model is run at a horizontal resolution of 2.0° × 0.5°. The ZC model has been routinely used for real-time ENSO forecasting since 1986 and has been widely applied in predictability studies (Blumenthal 1991; Xue et al. 1997; Xu and Duan 2008). The model describes the essential physics of ENSO and is appropriate for investigating the spring predictability barrier of ENSO.

a. CNOP-P errors for El Niño events in the Zebiak–Cane model

The empirical parameters in both atmospheric and oceanic components of the ZC model have the potential to yield model error and thereby affect the prediction skill of ENSO events. In this case, to what extent do the uncertainties in these empirical parameters affect ENSO predictability? Do the uncertainties cause a significant SPB for El Niño events? To answer these questions, we use the CNOP approach to find the optimal parameter error—that is, the CNOP-P error.

The ZC model contains nine main empirical parameters, which are listed in Table 1 along with their physical meanings and reference values (for details, see Zebiak and Cane 1987). Next, we calculate the CNOP-P errors of these parameters.

TABLE 1. Nine main parameters in the ZC model with their physical meanings, reference values, and the bounds of the constraint adopted in calculating the CNOP-P errors. The error bound $\sigma_i = x_i(\%)P_i$ is described as the percentage of the parameter error σ_i in the reference value P_i. The error bound column lists the values of "$x_i(\%)$" (see section 3a).

Parameter	Physical meaning	Reference values	Error bound (%)
α	Controlling strength of the SST-related component of atmospheric heating	1.6	0.1
β	Controlling strength of the convergence feedback portion of atmospheric heating	0.75	4
ε	Atmospheric friction parameter	0.3	0.3
η	Affecting surface heat flux (linear damping on SSTA)	0.98	0.02
T_1	$h > 0$, affecting the amplitude of subsurface temperature anomalies for positive h perturbations	28.0	0.1
b_1	$h > 0$, affecting the nonlinearity of subsurface temperature anomalies for positive h perturbations	1.25	1
T_2	$h < 0$, affecting the amplitude of subsurface temperature anomalies for negative h perturbations	−40.0	3
b_2	$h < 0$, affecting the nonlinearity of subsurface temperature anomalies for negative h perturbations	3.0	2
σ	Controlling the strength of wind stress	0.0329	1

A nonlinear optimization problem related to CNOP-P, $\mathbf{p}'_{\sigma,p}$, is defined as follows:

$$J(\mathbf{p}'_{\sigma,p}) = \max_{\mathbf{p}' \in C_\sigma} \|\mathbf{T}'(\tau)\|_2, \tag{9}$$

where $\mathbf{p}' = \{p'_1, p'_2, \ldots, p'_9\}$ describe the errors superimposed on the nine parameters P_i, $i = 1, 2, \ldots, 9$ (see Table 1), $\mathbf{p}' \in C_\sigma$ is the constraint of the parameter errors, and the cost function $\|\mathbf{T}'(\tau)\|_2 = \sqrt{\sum_{i,j}[T'_{i,j}(\tau)]^2}$ measures the magnitude of the prediction error of the SSTA at prediction time τ, as induced by parameter errors. Here $T'_{i,j}(\tau)$ represents the prediction error of the SSTA at different grid points, and (i, j) is the grid point in the domain of the tropical Pacific with a latitude and longitude from 19°S to 19°N (at an interval of 2°) and from 129.375°E to 84.375°W (at an interval of 5.625°), respectively. The prediction error $T'_{i,j}(\tau)$ of the SSTA can be obtained by subtracting the SSTA of the reference state El Niño events with the reference values of the parameters (see Table 1) from the predicted SSTA with perturbed parameters.

The constraint $\mathbf{p}' \in C_\sigma$ is chosen as $\{\mathbf{p}' \,|\, |p'_1| \le \sigma_1, |p'_2| \le \sigma_2, \ldots, |p'_9| \le \sigma_9\}$, where σ_i is a positive real number and represents an error bound. The constraint condition limits the magnitude of the error of each parameter, with $|p'_i| \le \sigma_i$; that is, $-\sigma_i \le p'_i \le \sigma_i$. In this paper, we determine the constraint bound according to the basic rules of the numerical simulation of ENSO. In realistic ENSO predictions, it should first be guaranteed that the forecast model can simulate the main features of the observed ENSO and at least avoid the occurrence of damping oscillation or departure from the climatology (Fig. 1). As such, the values of the parameters in the model must be set to satisfy this precondition. In satisfying this requirement, we found that the parameter errors satisfy the constraint condition, $-x_i(\%)P_i \le p'_i \le x_i(\%)P_i$, within which the corresponding disturbed parameters still produce persistent simulated ENSO events with an irregular oscillation (period 3–5 yr), without a damping oscillation or a departure from the climatology. In Table 1, the right-hand column ("error bound") lists the values of "x_i" under the constraint condition. The error bound $\sigma_i = x_i(\%)P_i$ is described as the percentage of parameter error in the reference value P_i, as shown in Table 1. For example, the reference value of the parameter β in the ZC model is 0.75, and its error is limited to the interval $[-0.75 \times 4\%, 0.75 \times 4\%]$, where the number 4 is the value of x_i in the constraint condition.

In this paper, the solver SQP (Powell 1982) is used to compute the CNOP-P error in the optimization problem shown in Eq. (9). As mentioned above, we need to calculate the gradient of the cost function with respect to parameter perturbations, for which the adjoint model is

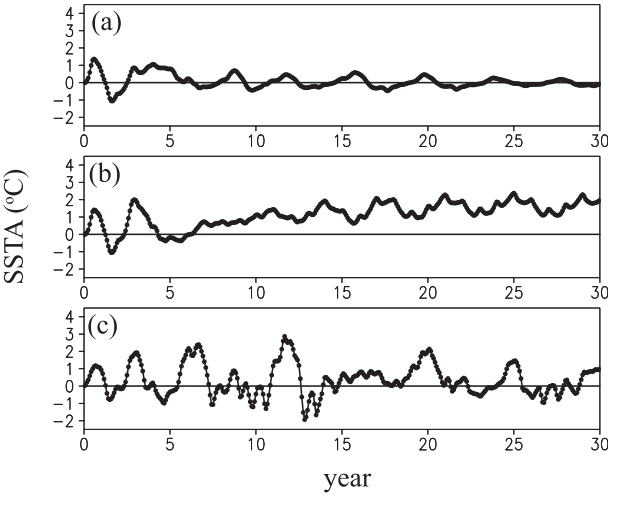

FIG. 1. SSTA component of two examples of ENSO 30-yr simulations with parameter perturbations that lie outside of the constraint: (a) β increased by 5% and the other parameters left unchanged; the amplitude of the ENSO oscillation shows a gradual decrease and (b) ε reduced by 0.4% and the other parameters left unchanged; a climate drift is observed. (c) All parameters were left unchanged; the ENSO oscillation is irregular.

an efficient tool. Xu and Duan (2008) constructed a tangent linear model of the ZC model and its corresponding adjoint model. To compute the CNOP-P error, we modified the adjoint of the ZC model according to Mu et al. (2010). Using this modified adjoint model, the gradient of the cost function with respect to parameter perturbations is computed, and the CNOP-P error can be obtained by the SQP solver. In calculating the CNOP-P error, as mentioned in section 2, we modify the maximization problem shown in Eq. (9) into a minimization one. Thirty initial guesses of the parameter perturbations are randomly generated. If several initial guesses converge to a point in the parametric phase space, this point can be considered the minimum in the neighborhood; thus, several such points are obtained, among which the point that yields the highest cost function in Eq. (9) is regarded as the CNOP-P error.

Sixteen model El Niño events are chosen as reference states for investigating the SPB phenomenon, which indicates that we will perform experiments in a perfect model scenario. These events include both strong and weak El Niño events with different initial warming times, which tend to peak at the end of the year. For each of these events, we made predictions based on a 12-month lead time, starting from different months of the year. Here, we use year (0) to denote the year when El Niño attains a peak value, and year (−1) and year (1) to signify the years before and after year (0), respectively. In numerical experiments, the El Niño predictions are first made with starting months of July (−1) [i.e., July in year (−1)], October (−1), January (0), and April (0). These four predictions start in the season before and extend through boreal spring in the growth phase of El Niño. For convenience, we refer to these predictions as growth-phase predictions. We performed further numerical experiments for El Niño predictions with starting months of July (0), October (0), January (1), and April (1). These four predictions cover the boreal spring in the decaying phase of El Niño; consequently, they are referred to as decaying-phase predictions. In total, eight predictions are made for each El Niño event, with eight starting months.

To investigate whether a significant SPB occurs in the predictions generated by the ZC model with disturbed model parameters, we analyzed the CNOP-P errors, for which the initial times are the predetermined starting months of the El Niño forecasting and the time interval is 12 months (i.e., $\tau = 12$ months, corresponding to a lead time of 12 months for the El Niño prediction). The initial conditions of the prediction experiments are the states of 16 model El Niño events at the starting months, which indicates the initial conditions being perfect and then allows us to study the effect of model parameter errors on prediction uncertainties. The error bounds related to the CNOP-P error are predetermined (see Table 1) according to the simulation rule outlined above. Eight predictions were made for each of the 16 El Niño events, yielding a total of 128 predictions. For each prediction, we computed the corresponding CNOP-P error. The computations revealed that for each prediction (whether for a strong or weak El Niño event), there is one CNOP-P error. Thus, a total of 128 CNOP-P errors were obtained. Furthermore, these CNOP-P errors correspond to the parameter perturbations that lie on the boundary of the domain defined by the constraint. Table 2 provides data for two examples of the CNOP-P errors, corresponding to predictions with starting months of July (−1) and July (0) for a particular El Niño event.

TABLE 2. CNOP-P errors of two predictions for a single El Niño event for starting months of July (−1) and July (0). The errors are expressed as a percentage of the corresponding reference value. The reference values of the parameters are listed in Table 1.

Parameter	Starting month July (−1)	Starting month July (0)
α	$0.1(\%)\alpha$	$-0.1(\%)\alpha$
β	$-4(\%)\beta$	$4(\%)\beta$
ε	$-0.3(\%)\varepsilon$	$0.3(\%)\varepsilon$
η	$0.02(\%)\eta$	$-0.02(\%)\eta$
T_1	$0.1(\%)T_1$	$-0.1(\%)T_1$
b_1	$-1(\%)b_1$	$1(\%)b_1$
T_2	$-3(\%)T_2$	$2.8(\%)T_2$
b_2	$2(\%)b_2$	$2(\%)b_2$
σ	$1(\%)\sigma$	$-1(\%)\sigma$

As stated in the introduction, a significant SPB, from the viewpoint of error growth, is considered to exist in ENSO forecasting with a large prediction error, with the error growth being especially large in spring. The CNOP-P errors cause the largest prediction uncertainty in the scenario of perfect initial fields, indicating that they may have the potential to induce the SPB phenomenon. If the CNOP-P errors do not cause a SPB for El Niño events, we could conclude that none of the parameter errors causes an SPB in the ZC model. Therefore, to investigate whether the parameter errors are related to a significant SPB, it is first necessary to estimate the seasonal growth tendencies of prediction errors caused by CNOP-P errors.

b. *Seasonal growth tendencies of prediction errors induced by CNOP-P errors*

We divided a calendar year into four seasons: January–March (JFM), April–June (AMJ), July–September (JAS), and October–December (OND). We computed the growth tendency of the prediction error with $\kappa \approx (\|\mathbf{T}'(t_2)\|_2 - \|\mathbf{T}'(t_1)\|_2)/(t_2 - t_1)$, where $\|\mathbf{T}'(t_1)\|_2$ and $\|\mathbf{T}'(t_2)\|_2$ represent the prediction errors of the SSTA

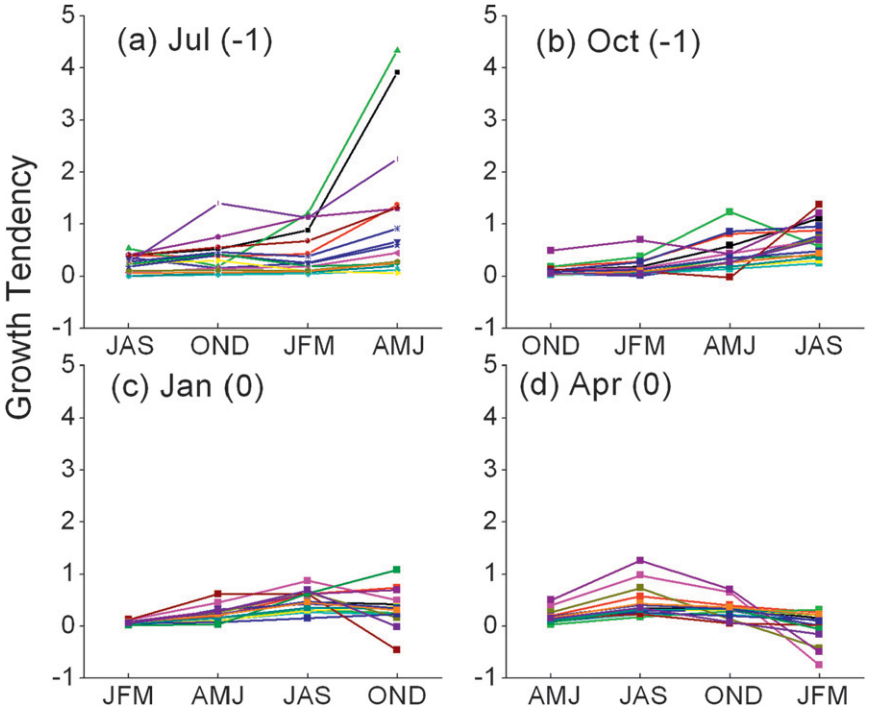

FIG. 2. Seasonal growth tendencies of prediction errors for 16 El Niño events caused by CNOP-P errors. Each line corresponds to one El Niño event. The prediction starting months are (a) July (−1), (b) October (−1), (c) January (0), and (d) April (0).

at the start of a season and at the end of the season and κ describes the error growth during a unit time (here the unit time is one season). Since each season possesses a common time interval length, we simply use the values of $\|\mathbf{T}'(t_2)\|_2 - \|\mathbf{T}'(t_1)\|_2$ to indicate the growth tendency κ for each season. A positive (negative) value of κ corresponds to an increase (decrease) of the prediction errors in that season, and the larger the absolute value of κ, the faster the increase (decrease) of the prediction errors in that season.

As described in section 3a, predictions starting from July (−1), October (−1), January (0), and April (0) cross the boreal spring (AMJ) in the growth phase of the El Niño event and are referred to as growth-phase predictions. In these predictions, the 16 El Niño events are each predicted for one year by integrating the ZC model for 12 months with a perfect initial field (i.e., the state of the El Niño events at the starting month) and a parametric field disturbed by the CNOP-P errors. The time-dependent prediction errors caused by the CNOP-P errors are obtained by subtracting the SSTA of the reference state El Niño event from those of the predicted El Niño events. The seasonal growth tendencies κ are then evaluated according to the prediction errors.

Figure 2 shows the seasonal growth tendencies κ for 16 El Niño events. For a starting month of July (−1) (Fig. 2a), although the largest κ induced by the CNOP-P errors tends to appear in the AMJ season, most predictions yield an indistinctive error increase in this season. Furthermore, for predictions with starting months of October (−1) (Fig. 2b), January (0) (Fig. 2c), and April (0) (Fig. 2d), the prediction errors of most of the predictions show the largest increases in JAS or OND. It is clear that the largest κ caused by CNOP-P errors does not always occur in AMJ; furthermore, the κ is very small, which results in a small prediction error for the El Niño events (Fig. 3). Although we investigated the seasonal growth tendencies for strong and weak El Niño events (16 events in total), we found no systematic difference between strong and weak events; that is, the results obtained when considering parameter errors are similar for both types of events.

We also investigated the decaying-phase predictions. For the eight predictions of each El Niño event, those with starting months of July (0), October (0), January (1), and April (1) cross the spring season during the decaying phase of the El Niño events. As before, we investigated the seasonal growth tendencies of prediction errors caused by the CNOP-P errors related to these decaying-phase predictions. For the 16 chosen El Niño events, the CNOP-P errors were obtained in section 3a. Regarding the κ related to these CNOP-P errors, the prediction

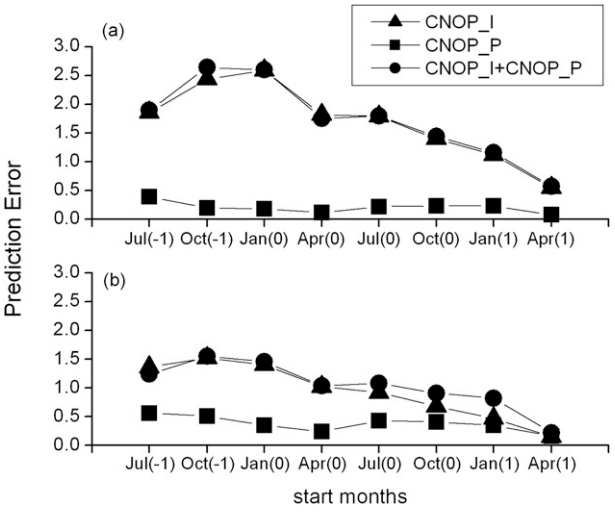

FIG. 3. (a) Ensemble mean of prediction errors for 16 El Niño events with a lead time of 12 months at each starting month, as measured using the absolute value of Niño-3 SSTA: (a) prediction errors caused by the corresponding CNOP-I errors, CNOP-P errors, and their combined mode with the initial constraint $\|\mathbf{u}_0\|_\alpha \le 0.8$ and parametric constraint with the error bound as listed in Table 1; (b) as in (a) but for the initial constraint $\|\mathbf{u}_0\|_\alpha \le 0.4$ and a parametric constraint that is double the error bound listed in Table 1.

errors show an inconspicuous season-dependent evolution and cause a small prediction error, generating a weakened SPB. Given that these findings are consistent with those of the growth-phase predictions, the relevant figures are omitted. The results indicate that the parameter errors are not the main contributing errors to the significant SPB for El Niño predictions generated by the ZC model.

The predictions generated by the ZC model with perturbed model parameters show that the model parameter errors do not possess an obvious season-dependent evolution of prediction errors and do not cause a large prediction error. However, Mu et al. (2007b), Yu et al. (2009), and Duan et al. (2009) demonstrated that initial errors with a particular spatial pattern could yield a large prediction error, causing a significant SPB for El Niño events. In fact, the CNOP-I errors are one such type of this kind of initial error. Therefore, it is important to consider whether an initial error is the dominant source of uncertainties that result in the development of a significant SPB. This question is addressed in the following section, based on a comparison of CNOP-I and CNOP-P errors.

4. Main source of uncertainties that cause a significant SPB for El Niño events in the ZC model

As mentioned above, Yu et al. (2009) demonstrated that CNOP-I errors cause a significant SPB. Yu et al. selected eight El Niño events with different initial warming times in computing the CNOP-I errors within the scenario of a perfect model. In the present study, to assess which errors play a dominant role in generating a significant SPB for El Niño events, we obtain the CNOP-I errors of the 128 predictions made for the 16 El Niño events selected for analysis. For details of the optimization problem and its calculation for CNOP-I errors, see the appendix or Yu et al. (2009). The resultant CNOP-I errors are similar to those reported by Yu et al. and can be classified into two types that possess a large-scale zonal dipolar pattern: one of the types has positive (negative) anomalies in the central (eastern) equatorial Pacific, while the locations of the anomalies are reversed for the other type (see Yu et al. 2009). In particular, CNOP-I errors are concentrated in a localized region of the equatorial central-western and eastern Pacific. The CNOP-I errors are computed for a constraint $\|\mathbf{u}_0\|_\alpha \le \delta$ with $\delta = 0.8$. From the resultant CNOP-I errors (Fig. 2 in Yu et al. 2009), we see that the CNOP-I errors within the localized region have SSTA errors < 0.08°C at each grid point, and the errors in the thermocline depth anomaly are < 2 m. However, the realistic analysis errors of the SSTA along the equator commonly possess a standard deviation of ~0.2°C (Kaplan et al. 1998; Dijkstra 2000), and Karspeck et al. (2006) estimated the analysis error of the thermocline depth anomaly to be < 15 m. It is conceivable that the magnitude of CNOP-I errors is smaller than that of a particular realistic analysis error, measured by an L2 norm; consequently, when the CNOP-I errors with the above constraint are projected to a particular realistic analysis error, the magnitude of the projected CNOP-I errors would be smaller in absolute terms than that of the analysis errors. Therefore, the initial constraint adopted here is acceptable for comparing the relative contributions of the initial error and the model parameter error in generating a significant SPB for El Niño events.

Figure 4 shows the ensemble mean of the seasonal growth tendencies induced by CNOP-P and CNOP-I errors associated with the growth-phase predictions for the 16 El Niño events. By comparing the ensemble mean of κ in four seasons, we can find that the CNOP-I errors of the predictions with a starting month of July (-1) and October (-1) have the largest κ in AMJ and show an obvious season-dependent evolution. For El Niño predictions with a starting month of January (0), the largest increases of CNOP-I errors are seen in JAS. For this situation, Mu et al. (2007b) argued that, although the largest increase of initial errors occurs in JAS, the error increase during AMJ is also large and may have caused the drastic decrease in El Niño forecast skill during

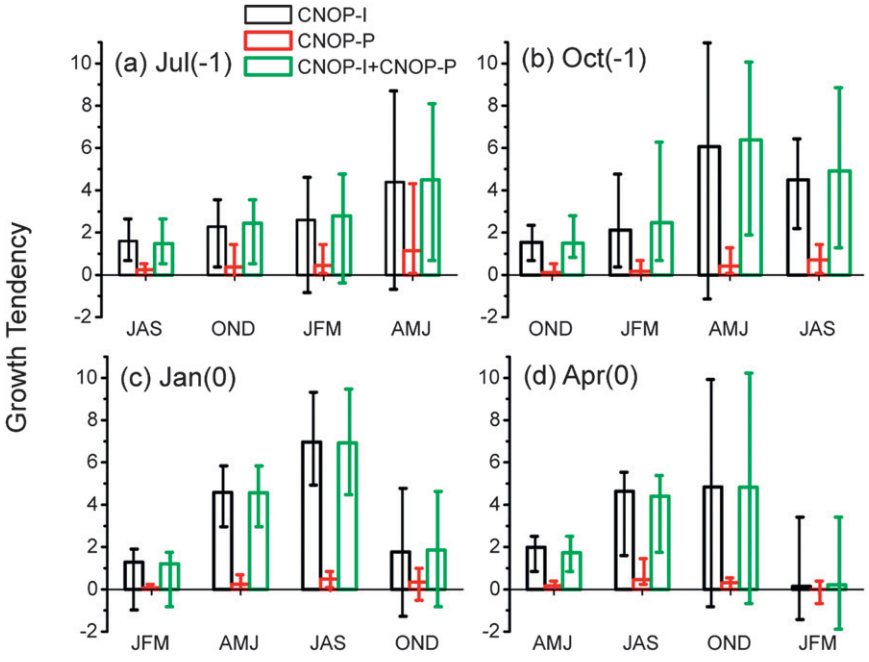

FIG. 4. Ensemble mean of the seasonal growth tendencies of prediction errors for 16 El Niño events, as caused by CNOP-I errors (black bars), CNOP-P errors (red bars), and their combined mode (green bars). To demonstrate spread of the ensemble, the maximal and minimal seasonal growth tendencies for 16 El Niño events are presented as a line segment along with each bar that represents the ensemble mean value. The starting months of the predictions are (a) July (−1), (b) October (−1), (c) January (0), and (d) April (0).

spring. Therefore, the CNOP-I errors of the growth-phase predictions with the above three starting months exhibit a prominent season-dependent evolution (see also Yu et al. 2009). However, we also demonstrated that the CNOP-P errors are associated with a less significant season-dependent evolution of prediction errors (see section 3a). Furthermore, for almost every season, the κ associated with the CNOP-P errors is notably smaller than that related to the CNOP-I errors; consequently, the prediction errors at prediction time caused by CNOP-I errors are much larger than those caused by CNOP-P errors (Fig. 3). For a starting month of April (0), significant increase of CNOP-I errors occurs mainly in OND. For CNOP-P errors, in contrast, the resultant prediction errors show a low increase in all seasons; consequently, they are much smaller than the prediction errors caused by CNOP-I errors.

The above results show that the CNOP-P errors, within a reasonable error bound, do not cause a large prediction error and do not induce a significant season-dependent evolution of prediction errors; therefore, they do not generate a significant SPB for El Niño events. The CNOP-I errors are more likely to cause a notable SPB than are the CNOP-P errors. This finding indicates that initial errors may play a dominant role in generating a significant SPB for El Niño events in the ZC model.

We also note that the growth behavior of the initial error is sensitive to the intensity of the El Niño event. The initial error growth for strong El Niño events is strongly affected by nonlinear processes, whereas a minor nonlinearity is found for weak El Niño events [as also reported by Yu et al. (2009)]. Given that these results are outside the scope of this paper, they are not described in detail.

We obtained similar results for the decaying-phase predictions as for the growth-phase predictions. That is, the CNOP-I errors cause a significant SPB, but the CNOP-P errors do not show an obvious season-dependent evolution of prediction errors. Therefore, initial errors may be the main source of uncertainties that cause a significant SPB for El Niño events.

Above, we compared the CNOP-I and CNOP-P errors, and concluded that the model parameter errors may not be a major source of uncertainties that cause a significant SPB for El Niño events. Note that the CNOP-I errors are related to the perfect model scenario, while the CNOP-P errors are associated with the perfect initial field scenario. However, in realistic predictions, initial errors and model parameter errors coexist in the forecast model. Therefore, to identify the errors that play a major role in generating a significant

SPB, it is necessary to further investigate the predictions for which both initial and model parameter errors exist.

Here, we explore the seasonal evolution of the prediction error caused by the combined mode of initial and model parameter errors and compare the results with the seasonal evolution of the prediction error caused by model parameter errors and by initial errors, respectively. This analysis supports the proposal that initial errors (rather than model parameter errors) are more likely to cause a significant SPB for El Niño events.

In these experiments, we used the ZC model with perturbed initial conditions and model parameters to predict the 16 selected El Niño events and to estimate their season-dependent predictability. In particular, we superimposed the CNOP-I errors and CNOP-P errors obtained above in the ZC model and integrated the model with a lead time of 12 months to obtain the prediction errors. Consequently, the prediction errors are caused by the combined mode of CNOP-I and CNOP-P errors.

The resultant prediction errors show an obvious season-dependent evolution for the 16 El Niño events and are much larger than those caused by the CNOP-P errors but are similar to those caused by the CNOP-I errors (Figs. 3 and 4). It is inferred that the initial error plays the dominant role in generating a significant SPB for El Niño events, which is consistent with the results of the comparison between the CNOP-I and CNOP-P errors (see above).

To this point, we have shown that CNOP-I errors with the constraint $\|\mathbf{u}_0\|_\alpha \le 0.8$ [see the appendix or Yu et al. (2009)] are more likely to yield a significant SPB for El Niño events in the ZC model than are CNOP-P errors with the constraint $|p_i'| \le \sigma_i, i = 1, 2, \ldots, 9$ (values of σ_i are listed in Table 1; see section 3). One might question whether these results reflect an excessively large initial error or excessively small parameter errors, even though the constraints have been clarified to lie within a reasonable error bound. To remove all doubts of this kind, we performed another group of predictability experiments as follows.

We take the δ value of the initial constraint $\|\mathbf{u}_0\|_\alpha \le \delta$ to be 0.4 (half of $\delta = 0.8$) and the σ_i value of the parameter error constraint $|p_i'| \le \sigma_i, i = 1, 2, \ldots, 9$, which are double the error bounds listed in Table 1. These magnitudes of parameter errors will cause a climate drift of the ENSO oscillation; however, we assess the degree to which these magnitudes of parameter errors affect the El Niño predictions with a lead time of one year.

Using the modified constraints outlined above, the CNOP-I and CNOP-P errors are computed to estimate the effect of model parameter errors on El Niño predictions. A comparison of the prediction errors caused by CNOP-I, CNOP-P, and the combined mode of the CNOP-I and CNOP-P errors revealed that, in most cases, the CNOP-P errors with a larger magnitude (in terms of the chosen measurement) still yield a small prediction error of the Niño-3 SSTA, but the CNOP-I errors with a smaller magnitude cause a large prediction error (Fig. 3); furthermore, the small magnitude of CNOP-I errors shows an obvious season-dependent evolution, whereas the large magnitude of CNOP-P errors shows a less significant season-dependent evolution. Moreover, the prediction errors caused by the combined mode of CNOP-I and CNOP-P errors have a similar magnitude to those caused by the CNOP-I errors (Fig. 3).

The above results indicate that an increase in the error bound of parameter errors or a decrease in the error bound of initial errors does not affect the conclusion that the initial error plays a dominant role in the occurrence of a significant SPB. To further illustrate this result, we investigated the spatial pattern of the seasonal evolution of predicted SSTA. The CNOP-I errors and the combined mode of CNOP-I and CNOP-P errors have greater potential than the CNOP-P errors in terms of disrupting the evolution of the reference state El Niño events (e.g., see the predictions in Fig. 5). Figure 5 shows that differences between the predicted SSTA patterns associated with the CNOP-I errors (and the combined mode of CNOP-I and CNOP-P errors) and SSTA patterns of the reference state El Niño events tend to increase significantly during AMJ. However, it should be noted that, although the prediction error caused by CNOP-I error evolves more dramatically in magnitude than that caused by CNOP-P errors, both prediction errors bear a similar pattern to some extent after several months, especially after a half-year evolution. Figure 6 shows the spatial pattern of the SSTA component of prediction errors caused by these two kinds of errors associated with the El Niño prediction as in Fig. 5 and their monthly similarity coefficients. It is shown that the negative similarity coefficients, after six months, approach -1 over time, which suggests that the SSTA spatial patterns of the resultant two prediction errors bear more and more similarities despite having opposite signs. Of course, there also exists other El Niño predictions whose time-dependent prediction errors caused by the CNOP-I errors and CNOP-P errors possess similar patterns with common signs after 6 months but with significant differences in error magnitudes. In any case, for the prediction errors caused by the CNOP-I errors and CNOP-P errors, they have similar patterns but with considerable differences in error magnitudes, which implies that the differences between CNOP-I errors and CNOP-P errors in the ZC model mainly lie in the magnitudes of their resultant prediction errors, not

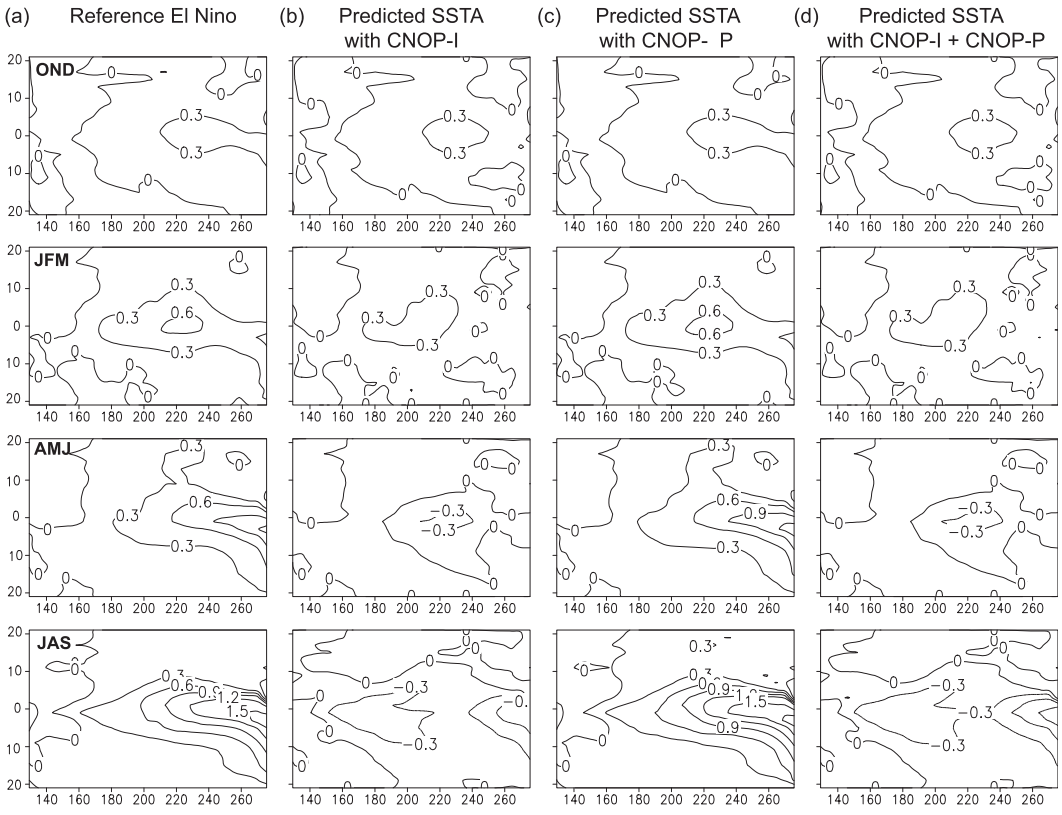

FIG. 5. SSTA component of the seasonal evolution of (a) the reference state El Niño event with initial warming in July (−1), (b) the predicted El Niño with CNOP-I error, (c) the predicted El Niño with CNOP-P error, and (d) the predicted El Niño with the combined mode of the CNOP-I and CNOP-P errors. The predictions are made from October (−1).

the structure. This also illustrates that initial errors, compared to model parameter errors, are likely to cause large prediction errors and play a dominant role in yielding uncertainties for El Niño predictions bestriding boreal spring.

From the above results, we have demonstrated that the initial errors, rather than the model parameter errors, are likely to cause a significant SPB for El Niño events. Of course, these results were derived solely from the ZC model and need to be further validated using additional models. It is also necessary to investigate a more realistic error constraint. Despite these limitations, the present results provide important information on El Niño predictions.

5. Summary and discussion

In this paper, we applied the approach of conditional nonlinear optimal perturbation (CNOP) in the Zebiak–Cane model (ZC model) to study the effect of parameter errors on El Niño predictability and to identify the errors that play a dominant role in generating a significant SPB for El Niño events. Note that reasonable error bounds for the parameters were predetermined based on the assumption that model parameter errors are small enough to avoid climate drift of ENSO oscillations. With reasonable constraint conditions, the CNOP initial errors (CNOP-I) and CNOP parameter errors (CNOP-P) were obtained. The CNOP-I errors, in perfect model experiments, act as the optimal initial errors, and the CNOP-P errors, in perfect initial condition experiments, represent the optimal parameter errors. In their respective scenarios, they cause the largest prediction error. A comparison of the prediction errors caused by the CNOP-I and CNOP-P errors revealed that the CNOP-P errors do not give rise to a noticeable prediction error of the Niño-3 sea surface temperature anomaly (SSTA) and do not show an obvious season-dependent evolution of prediction errors. In contrast, the CNOP-I errors cause a large prediction error and tend to have an obvious season-dependent evolution, with the largest error increase in spring. Therefore, the initial errors, rather than the parameter errors, play a dominant role in generating a significant SPB for

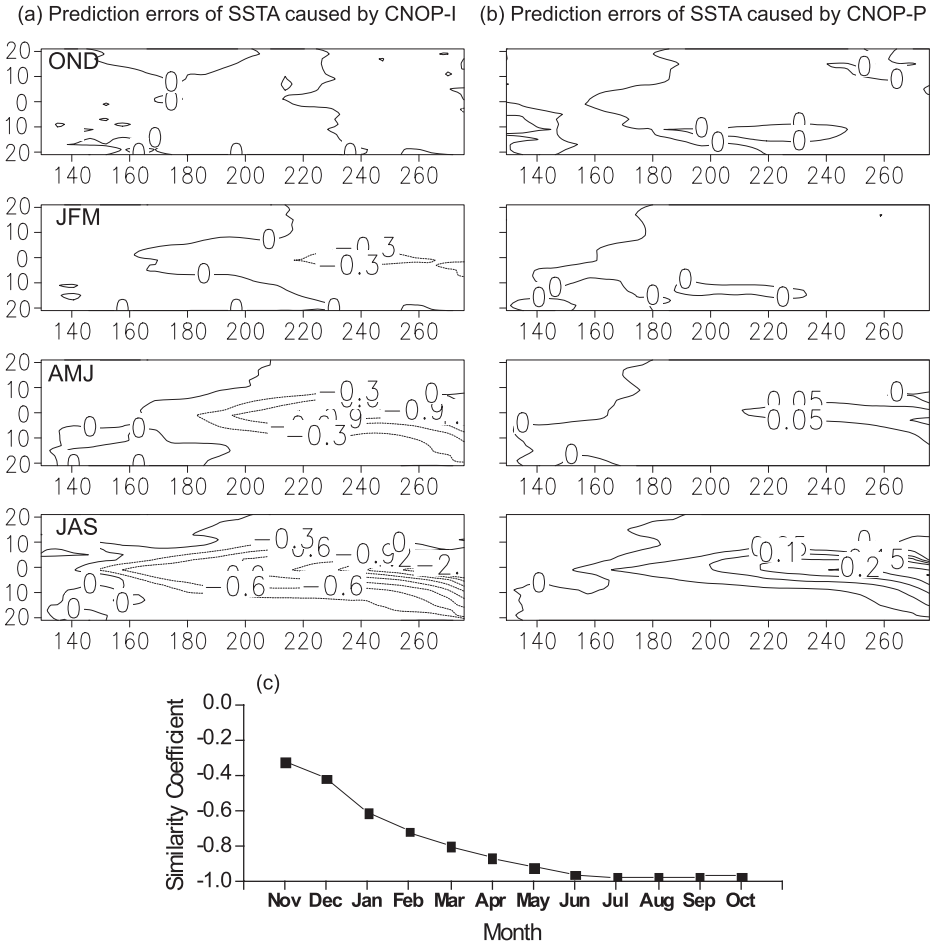

FIG. 6. Seasonal evolution of prediction errors of SSTAs caused by (a) CNOP-I error and (b) CNOP-P error associated with the El Niño predictions as in Fig. 5: counter interval 0.3 is for (a) and 0.05 for (b). (c) Time-dependent similarity coefficients between the patterns of the SSTA component of the prediction errors caused by the CNOP-I and CNOP-P errors.

El Niño events. To further validate this result, an experiment was performed to investigate the situation in which the CNOP-I and CNOP-P errors are simultaneously superimposed in the model, which may be more plausible because the initial errors and model parameter errors coexist in realistic predictions. The combined mode of CNOP-I and CNOP-P errors showed a similar season-dependent evolution to that of CNOP-I errors and also yielded a large prediction error, in contrast to the CNOP-P errors. Therefore, it is inferred that the initial errors (rather than model parameter errors) play a dominant role in generating a significant SPB for El Niño predictions of the ZC model. A smaller magnitude of initial errors and a larger magnitude of parameter errors were also used to investigate the relative effect of initial errors and model parameter errors on a significant SPB for El Niño events. The corresponding results support the above conclusion and emphasize the role of initial errors in generating a significant SPB. These results provide a clue as to why Chen et al. (1995, 2004) achieved a significant reduction in the SPB phenomenon by improving the initialization of the forecast model. The results also indicate the importance of data assimilation in ENSO predictions.

This paper investigated the effect of model errors on a significant SPB based on model El Niño events and only considered the role of model parameter errors in the SPB. Previous studies that used the stochastic optimal approach to investigate ENSO predictability (Kleeman and Moore 1997; Moore and Kleeman 1999) explored the influence of stochastic noise forcing on ENSO predictability, which is another type of model error in addition to those considered in the present study. It is well known that model errors are derived from various sources, including parameter errors, external forcing, and different types of physical parameterization schemes. We

used the ZC model to show that the model parameter errors fail to cause a significant SPB. However, it is unknown whether other types of model errors cause a significant SPB and which type of model error has the largest effect on ENSO predictability. It is necessary to address these questions in future works and to thereby provide information to modelers that will enable the improvement of forecast models.

Because the main characteristics of La Niña events (e.g., phase locking) are poorly reproduced by the Zebiak–Cane model (An and Wang 2001), we made no attempt to study the corresponding problem for La Niña events. We anticipate that more realistic ENSO models can be used to investigate the SPB for ENSO events, for the purpose of identifying the differences in predictability of El Niño and La Niña. Given the limitations of existing algorithms, it is difficult to use the CNOP approach to tackle predictability problems related to spatially varying parameters. Therefore, a more effective algorithm is required. In addition, we performed forecast experiments with scenarios such as perfect model or perfect initial field so as to identify the major source of the uncertainties that causes a significant SPB for El Niño events. The reference El Niño events were also from model El Niño events. In a word, the forecast experiments in this study are performed with a few assumptions and are different from realistic El Niño predictions. A realistic forecast experiment strategy should be designed to examine the theoretical conclusions obtained in this study.

The SPB for ENSO is an unresolved problem, although it has attracted the attention of many scientists. This paper investigated the effect of parameter errors on SPBs and compared them with the effect of initial errors, demonstrating the importance of initial errors in generating a significant SPB. However, there are questions that remain to be addressed. For example, which physical variables are most sensitive to perturbations in the initial fields and in the model parameters? Do the optimal perturbations provide information in terms of identifying those parameters that should be better constrained by observations? As stated above, do other types of model errors cause a significant SPB? Which type of model error should be minimized to improve the forecast skill? Furthermore, the mechanism by which the SPB develops remains debatable despite many hypotheses proposed to explain its occurrence (Webster and Yang 1992; Mu et al. 2007a). These topics are worthy of attention in future studies.

Acknowledgments. We appreciate the three reviewers for their valuable comments. This work was jointly sponsored by the Knowledge Innovation Program of the Chinese Academy of Sciences (Grant KZCX2-YW-QN203), the National Nature Scientific Foundation of China (Grants 41006015 and 41176013), the National Basic Research Program of China (Grant 2010CB950402), and the Basic Research Program of Qingdao Scientific and Technological Plan (Grant 111495jch).

APPENDIX

CNOP-I Errors for El Niño Events in the Zebiak–Cane Model

The CNOP-I errors, denoted by $\mathbf{u}_{0\delta,I}$, are obtained by solving the following nonlinear optimization problem:

$$J(\mathbf{u}_{0\delta,I}) = \max_{\|\mathbf{u}_0\|_\alpha \le \delta} \|\mathbf{T}'(\tau)\|_2, \tag{A1}$$

where $\mathbf{u}_0 = (w_1^{-1}\mathbf{T}'_0, w_2^{-1}\mathbf{h}'_0)$ is a nondimensional initial error of the SSTA and thermocline depth anomaly superimposed on the initial state of a predetermined reference state El Niño event: $w_1 = 2°C$ and $w_2 = 50$ m are characteristic scales of SST and thermocline depth. The constraint condition is $\|\mathbf{u}_0\|_\alpha \le \delta$, and the norm is $\|\mathbf{u}_0\|_\alpha = \sqrt{\sum_{i,j}[(w_1^{-1}T'_{0i,j})^2 + (w_2^{-1}h'_{0i,j})^2]}$, where $T'_{0i,j}$ and $h'_{0i,j}$ represent the dimensional initial error of the SSTA and thermocline depth anomaly at different grid points, and (i, j) is the grid point in the domain of the tropical Pacific from 19°S to 19°N (at an interval of 2°), 129.375°E to 84.375°W (at an interval of 5.625°) and. The evolution of the initial error is measured by $\|\mathbf{T}'(\tau)\|_2 = \sqrt{\sum_{i,j}[T'_{i,j}(\tau)]^2}$; $\mathbf{T}'(\tau)$ represents the prediction error of SSTA at time τ and is obtained by subtracting the SSTA of the reference state from the predicted SSTA with initial errors at prediction time τ. Note that there is only one variable SSTA to be used to measure the prediction errors of an El Niño event, while both SST and thermocline depth anomalies are considered in the initial errors. It is known that if a Niño-3 SSTA larger than 0.5°C persists for 6 months, it is regarded as an El Niño event; that is to say, the onset of an El Niño event is generally determined by the magnitudes of the SSTA. Therefore, we use the error evolution for the SSTA to measure the prediction error of an El Niño event. For the factors that affect the evolution of El Niño, Wang and Fang (1996) demonstrated that the SST and thermocline depth anomalies are the two main physical components. Therefore, we consider the SSTA and thermocline depth anomaly components in the initial errors. This may illustrate that the errors superimposed on the SSTA and thermocline depth anomaly eventually affect the evolution of the SSTA through some positive or negative feedback mechanisms.

We use the SPG2 solver to obtain the CNOP-I of the ZC model. To obtain CNOP-I, we modify the corresponding maximization problem into a minimization one and try at least 30 initial guesses (obtained randomly). If several initial guesses converge to a point in the phase space, this point can be considered a minimum in the neighborhood; thus, several such points are obtained, of which the one that yields the largest cost function in Eq. (A1) is regarded as CNOP-I.

REFERENCES

An, S. I., and B. Wang, 2001: Mechanisms of locking the El Niño and La Niña mature phases to boreal winter. *J. Climate,* **14,** 2164–2176.

Birgin, E. G., J. M. Martínez, and M. Raydan, 2000: Nonmonotone spectral projected gradient methods on convex sets. *SIAM J. Optim.,* **10,** 1196–1211.

Blanke, B., J. D. Neelin, and D. Gutzler, 1997: Estimating the effect of stochastic wind stress forcing on ENSO irregularity. *J. Climate,* **10,** 1473–1486.

Blumenthal, M. B., 1991: Predictability of a coupled ocean–atmosphere model. *J. Climate,* **4,** 766–784.

Chen, D., S. E. Zebiak, A. J. Busalacchi, and M. Cane, 1995: An improved procedure for El Niño forecasting: Implications for predictability. *Science,* **269,** 1699–1702.

——, M. Cane, A. Kaplan, S. E. Zebiak, and D. J. Huang, 2004: Predictability of El Niño over the past 148 years. *Nature,* **428,** 733–736.

Dijkstra, H. A., 2000: *Nonlinear Physical Oceanography: A Dynamical Systems Approach to the Large Scale Ocean Circulation and El Niño*. Atmospheric and Oceanographic Sciences Library, Vol. 22, Kluwer Academic Publishers, 451 pp.

Duan, W., and M. Mu, 2006: Investigating decadal variability of El Niño–Southern Oscillation asymmetry by conditional nonlinear optimal perturbation. *J. Geophys. Res.,* **111,** C07015, doi:10.1029/2005JC003458.

——, and R. Zhang, 2010: Is model parameter error related to a significant spring predictability barrier for El Niño events? Result from a theoretical model. *Adv. Atmos. Sci.,* **27,** 1003–1013.

——, M. Mu, and B. Wang, 2004: Conditional nonlinear optimal perturbations as the optimal precursors for El Niño–Southern Oscillation events. *J. Geophys. Res.,* **109,** D23105, doi:10.1029/2004JD004756.

——, H. Xu, and M. Mu, 2008: Decisive role of nonlinear temperature advection in El Niño and La Niña amplitude asymmetry. *J. Geophys. Res.,* **113,** C01014, doi:10.1029/2006JC003974.

——, X. Liu, K. Zhu, and M. Mu, 2009: Exploring the initial errors that cause a significant "spring predictability barrier" for El Niño events. *J. Geophys. Res.,* **114,** C04022, doi:10.1029/2008JC004925.

Flugel, M., and P. Chang, 1998: Does the predictability of ENSO depend on the seasonal cycle? *J. Atmos. Sci.,* **55,** 3230–3243.

Gebbie, G., I. Eisenman, A. Wittenberg, and E. Tziperman, 2007: Modulation of westerly wind bursts by sea surface temperature: A semistochastic feedback for ENSO. *J. Atmos. Sci.,* **64,** 3281–3295.

Hao, Z., and M. Ghil, 1994: Data assimilation in a simple tropical ocean model with wind stress errors. *J. Phys. Oceanogr.,* **24,** 2111–2128.

Jin, E. K., and Coauthors, 2008: Current status of ENSO prediction skill in coupled ocean–atmosphere models. *Climate Dyn.,* **31,** 647–664.

Kaplan, A., M. Cane, Y. Kushnir, A. C. Clement, M. B. Blumenthal, and B. Rajagopalan, 1998: Analyses of global sea surface temperature 1856–1991. *J. Geophys. Res.,* **103,** 18 567–18 589.

Karspeck, A., A. Kaplan, and M. Cane, 2006: Predictability loss in an intermediate ENSO model due to initial error and atmosphere noise. *J. Climate,* **19,** 3572–3588.

Kirtman, B. P., 1997: Oceanic Rossby wave dynamics and the ENSO period in a coupled model. *J. Climate,* **10,** 1690–1704.

——, J. Shukla, M. Balmaseda, N. Graham, C. Penland, Y. Xue, and S. Zebiak, Eds., 2002: Current status of ENSO forecast skill: A report to the CLIVAR Working Group on seasonal to interannual prediction. WCRP Informal Rep. 23/01, ICPO Publ. 56, 26 pp.

Kleeman, R., 1991: A simple model of the atmospheric response to ENSO sea surface temperature anomalies. *J. Atmos. Sci.,* **48,** 3–18.

——, and A. M. Moore, 1997: A theory for the limitation of ENSO predictability due to stochastic atmospheric transients. *J. Atmos. Sci.,* **54,** 753–767.

Latif, M., A. Sterl, E. Maier-Reimer, and M. M. Junge, 1993: Structure and predictability of the El Niño/Southern Oscillation phenomenon in a coupled ocean–atmosphere general circulation model. *J. Climate,* **6,** 700–708.

——, and Coauthors, 1998: A review of the predictability and prediction of ENSO. *J. Geophys. Res.,* **103,** 14 375–14 393.

Lau, K. M., and S. Yang, 1996: The Asian monsoon and predictability of the tropical ocean-atmosphere system. *Quart. J. Roy. Meteor. Soc.,* **122,** 945–957.

Le Dimet, F. X., and O. Talagrand, 1986: Variational algorithms for analysis and assimilation of meteorological observations: Theoretical aspects. *Tellus,* **38A,** 97–110.

Liu, D. C., and J. Nocedal, 1989: On the limited memory method for large scale optimization. *Math. Programming,* **45B,** 503–528.

Liu, Z. Y., 2002: A simple model study of ENSO suppression by external periodic forcing. *J. Climate,* **15,** 1088–1098.

Lorenz, E. N., 1965: A study of the predictability of a 28-variable atmospheric model. *Tellus,* **17,** 321–333.

Lu, J., and W. W. Hsieh, 1998: On determining initial conditions and parameters in a simple coupled atmosphere-ocean model by adjoint data assimilation. *Tellus,* **50A,** 534–544.

Luo, J. J., S. Masson, S. Behera, and T. Yamagata, 2008: Extended ENSO predictions using a fully coupled ocean–atmosphere model. *J. Climate,* **21,** 84–93.

MacMynowski, D. G., and E. Tziperman, 2008: Factors affecting ENSO's period. *J. Atmos. Sci.,* **65,** 1570–1586.

Marshall, A. G., O. Alves, and H. H. Hendon, 2009: A coupled GCM analysis of MJO activity at the onset of El Niño. *J. Atmos. Sci.,* **66,** 966–983.

McCreary, J. P., and D. L. T. Anderson, 1991: An overview of coupled models of El Niño and the Southern Oscillation. *J. Geophys. Res.,* **96,** 3125–3150.

McPhaden, M. J., 2003: Tropical Pacific Ocean heat content variations and ENSO persistence barriers. *Geophys. Res. Lett.,* **30,** 1480, doi:10.1029/2003GL016872.

——, S. E. Zebiak, and M. H. Glantz, 2006: ENSO as an integrating concept in earth science. *Science,* **314,** 1740–1745.

Moore, A. M., and R. Kleeman, 1996: The dynamics of error growth and predictability in a coupled model of ENSO. *Quart. J. Roy. Meteor. Soc.,* **122,** 1405–1446.

——, and ——, 1999: Stochastic forcing of ENSO by the intraseasonal oscillation. *J. Climate,* **12,** 1199–1220.

Mu, M., and W. Duan, 2003: A new approach to studying ENSO predictability: Conditional nonlinear optimal perturbation. *Chin. Sci. Bull.,* **48,** 1045–1047.

——, ——, and J. Wan, 2002: The predictability problems in numerical weather and climate prediction. *Adv. Atmos. Sci.,* **19,** 191–204.

——, L. Sun, and D. A. Henk, 2004: The sensitivity and stability of the ocean's thermocline circulation to finite amplitude freshwater perturbations. *J. Phys. Oceanogr.,* **34,** 2305–2315.

——, W. Duan, and B. Wang, 2007a: Season-dependent dynamics of nonlinear optimal error growth and El Niño-Southern Oscillation predictability in a theoretical model. *J. Geophys. Res.,* **112,** D10113, doi:10.1029/2005JD006981.

——, H. Xu, and W. Duan, 2007b: A kind of initial errors related to ''spring predictability barrier'' for El Niño events in Zebiak-Cane model. *Geophys. Res. Lett.,* **34,** L03709, doi:10.1029/2006GL027412.

——, F. Zhou, and H. Wang, 2009: A method for identifying the sensitive areas in targeted observations for tropical cyclone prediction: Conditional nonlinear optimal perturbation. *Mon. Wea. Rev.,* **137,** 1623–1639.

——, W. Duan, Q. Wang, and R. Zhang, 2010: An extension of conditional nonlinear optimal perturbation approach and its applications. *Nonlinear Processes Geophys.,* **17,** 211–220.

Neelin, J. D., 1990: A hybrid coupled general circulation model for El Niño studies. *J. Atmos. Sci.,* **47,** 674–693.

Penland, C., and T. Magorian, 1993: Prediction of Niño 3 sea surface temperatures using linear inverse modeling. *J. Climate,* **6,** 1067–1076.

Powell, M. J. D., 1982: VMCWD: A Fortran subroutine for constrained optimization. DAMTP Rep. 1982/NA4, 13 pp.

Sun, L., M. Mu, D.-J. Sun, and X.-Y. Yin, 2005: Passive mechanism of decadal variation of thermohaline circulation. *J. Geophys. Res.,* **110,** C07025, doi:10.1029/2005JC002897.

Syu, H.-H., and J. D. Neelin, 2000: ENSO in a hybrid coupled model. Part I: Sensitivity to physical parameterizations. *Climate Dyn.,* **16,** 19–34.

Tang, Y., and B. Yu, 2008: MJO and its relationship to ENSO. *J. Geophys. Res.,* **113,** D14106, doi:10.1029/2007JD009230.

Terwisscha van Scheltinga, A. D., and H. A. Dijkstra, 2008: Conditional nonlinear optimal perturbations of the double-gyre ocean circulation. *Nonlinear Processes Geophys.,* **15,** 727–734.

Thompson, C. J., 1998: Initial conditions for optimal growth in a coupled ocean–atmosphere model of ENSO. *J. Atmos. Sci.,* **55,** 537–557.

van Oldenborgh, G. J., M. A. Balmaseda, L. Ferranti, T. N. Stockdale, and D. L. T. Anderson, 2005: Evaluation of atmospheric fields from the ECMWF seasonal forecasts over a 15-year period. *J. Climate,* **18,** 3250–3269.

Wang, B., and Z. Fang, 1996: Chaotic oscillation of tropical climate: A dynamic system theory for ENSO. *J. Atmos. Sci.,* **53,** 2786–2802.

Wang, C., and J. Picaut, 2004: Understanding ENSO physics—A review. *Earth Climate: The Ocean-Atmosphere Interaction, Geophys. Monogr.,* Vol. 147, Amer. Geophys. Union, 21–48.

Webster, P. J., and S. Yang, 1992: Monsoon and ENSO: Selectively interactive systems. *Quart. J. Roy. Meteor. Soc.,* **118,** 877–926.

Williams, P. D., 2005: Modelling the climate change: The role of unresolved process. *Philos. Trans. Roy. Soc. London,* **363,** 2931–2946.

Wu, D. H., D. L. T. Anderson, and M. K. Davey, 1993: ENSO variability and external impacts. *J. Climate,* **6,** 1703–1717.

Wu, X., and M. Mu, 2009: Impact of horizontal diffusion on the nonlinear stability of thermohaline circulation in a modified box model. *J. Phys. Oceanogr.,* **39,** 798–805.

Xu, H., and W. Duan, 2008: What kind of initial errors cause the severest prediction uncertainty of El Niño in Zebiak-Cane model. *Adv. Atmos. Sci.,* **25,** 577–584.

Xue, Y., M. A. Cane, and S. E. Zebaik, 1997: Predictability of a coupled model of ENSO using singular vector analysis. Part I: Optimal growth in seasonal background and ENSO cycles. *Mon. Wea. Rev.,* **125,** 2043–2056.

Yu, J.-Y., and H.-Y. Kao, 2007: Decadal changes of ENSO persistence barrier in SST and ocean heat content indices: 1958–2001. *J. Geophys. Res.,* **112,** D13106, doi:10.1029/2006JD007654.

Yu, Y., W. Duan, H. Xu, and M. Mu, 2009: Dynamics of nonlinear error growth and season-dependent predictability of El Niño events in the Zebiak–Cane model. *Quart. J. Roy. Meteor. Soc.,* **135,** 2146–2160.

Zavala-Garay, J., A. M. Moore, and R. Kleeman, 2004: Influence of stochastic forcing on ENSO prediction. *J. Geophys. Res.,* **109,** C11007, doi:10.1029/2004JC002406.

Zebiak, S. E., and M. Cane, 1987: A model El Niño–Southern Oscillation. *Mon. Wea. Rev.,* **115,** 2262–2278.

Zhang, L., M. Flügel, and P. Chang, 2003: Testing the stochastic mechanism for low-frequency variations in ENSO predictability. *Geophys. Res. Lett.,* **30,** 1630, doi:10.1029/2003GL017505.